Fibers and Polymers 2003, Vol.4, No.1, 15-19

A Molecular Dynamics Simulation on the Self-assembly of ABC Triblock Copolymers. 3. Effects of Block Composition in Asymmetric Triblock Copolymers†

Min Jae Ko, Seung Hyun Kim, and Won Ho Jo*

Hyperstructured Organic Materials Research Center and School of Materials Science and Engineering, Seoul National University, Seoul 151-742, Korea

(Received October 15, 2002; Accepted November 30, 2002)

Abstract: The self-assembly of asymmetric ABC triblock copolymers in the ordered structure is investigated using an isothermal-isobaric molecular dynamics simulation. Unlike symmetric ABC triblock copolymers, more fascinating morphologies are observed in asymmetric ones because of a larger difference of incompatibility between the components. Various modes of self-assembly in assymmetric ABC triblock copolymers are also observed depending on the block composition. When the composition of block A is changed from 0.125 to 0.25 at the same $f_B = 0.25$, the morphological transition from the "cylinder in cylinder" to "cylinders at cylinder" structure is observed in the simulation. In the case of ABC triblocks with $f_B = 0.5$, a lamellar-type structure is changed to a cylinder-type structure with increasing the length of block A. When the mid-block length increases further to $f_B = 0.625$, the "spheres on cylinder" structure is observed in both the $A_{10}B_{50}C_{20}$ and $A_{20}B_{50}C_{10}$ triblocks. From these results, the phase diagram of ABC triblock copolymers can be constructed.

Keywords: Molecular dynamics, Self-assembly, ABC triblock copolymer, Block composition

Introduction

The self-assembly of AB diblock copolymer has been well understood owing to a number of experimental investigation [1-3] and theoretical approaches[4-6]. Furthermore, recent advances in synthetic chemistry have induced new attention to ABC triblock copolymers. However, a wide range of parameter space of ABC triblock copolymers makes it difficult to systematically study the self-assembly of ABC copolymers. As a result, the self-assembling behavior of ABC triblock copolymers has not been completely understood yet. In our previous studies[7,8], we investigated by molecular dynamics simulation the effect of block composition and sequence on the self-assembly of symmetric triblock copolymers. The simulation result showed that several different types of microphase separated structures were observed depending on the block composition and sequence. It is generally known that the morphology of ABC triblock copolymer is determined by thermodynamic balance between the three different blocks[9-18].

Asymmetric ABC triblock copolymers, in which both end blocks A and C have the different chain length, can provide more opportunities to yield a number of new interesting morphologies, because the differences between the lengths of two end blocks may change the degree of incompatibility between the components. A few unusual morphologies, which had not been observed in symmetric ABC triblocks, were found in asymmetric ones by Stadler group[10-12]. They reported that the helical microphase separated morphology was observed in an asymmetric PS-PB-PMMA triblock[10]. In the morphology, four small PB cylinders turn as a fourfold helix around a core cylinder of PS, while PMMA forms the matrix as the majority component. This novel structure is especially striking because it corresponds to the case in which there is no chirality at a molecular level, whereas a chiral structure develops in an assembly of the molecules. More recently, they also reported that the formation of cylindrical morphologies is governed by the sum of the volume fractions of A and B as well as by their ratio for asymmetric ABC triblock copolymers with the endblock C as the majority component[11]. In addition to the morphologies based on the cylindrical structure, the morphologies with spherical motif, such as "spheres on sphere" structure, have been reported in asymmetric PS-PB-PMMA triblock copolymers and the corresponding hydrogenated PS-PEB-PMMA ones[12].

In this paper, we report the composition effect on the morphology of asymmetric ABC triblock copolymers by using a molecular dynamic simulation. An isothermal-isobaric molecular dynamics simulation is used again here, since it has been proven from our previous studies to be a very powerful tool in understanding the self-assembly of ABC triblock copolymers.

Model and Simulation Method

The model of triblock copolymers and the simulation method employed in this work are detailed in our previous papers[7,8] and only the main points are summarized here. The simulation is performed based on the isothermal-isobaric ensemble, and a coarse grained model is employed

*Corresponding author: whjpoly@plaza.snu.ac.kr

†Dedicated to Professor Won-Jei Cho on the occasion of his retirement.

to simulate the triblock copolymer chain. In this model, each chain consists of N beads with identical size. Each bead is subject to the harmonic bond stretching potential and non-bonded Lennard-Jones (LJ) potential. The LJ energy parameter ε_{ij} for segments i and j, has the following relation, i.e., $\varepsilon_{AC} < \varepsilon_{AB} < \varepsilon_{BC}$. This relative magnitude of interaction parameters means that incompatibility between A and C is smaller than the incompatibility between A and B and between B and C blocks, and the interaction between B and C is the most unfavorable. This relation of interaction parameters corresponds qualitatively to the case of PS-PB-PMMA triblock copolymer where $\chi_{PS\text{-}PMMA} < \chi_{PS\text{-}PB} < \chi_{PB\text{-}PMMA}$.

All the triblock copolymers have a constant total chain length $N = 80$ and the volume fraction (f_B) of midblock is varied from 0.25 to 0.625. At each f_B, the chain length of end block A and C is systematically changed to investigate the composition effect. In this study, all the simulations are performed on the commercial modeling software, *Cerius*^{2} of Molecular Simulation Inc. The simulation procedure and various parameters are the same as our previous papers[7,8].

Results and Discussion

Simulated results for symmetric ABC triblock copolymers with various compositions are reported in our earlier publications[7,8]. In the present work, the morphologies of asymmetric ones are simulated and discussed by comparing simulated results with experimental ones. When the block copolymer of $A_{10}B_{20}C_{50}$ with $f_B = 0.25$ is simulated, the snapshot shows the cylindrical core-shell morphology, in which an inner cylinder consisting of block A is surrounded by a cylindrical shell of block B within the C matrix, as shown in Figure 1(a). The schematic description of this structure is shown in Figure 1(b). Here, the number in subscript of each block notation indicates the chain length of each block. The formation of this structure is explained in terms of the relative volume fraction and the relative magnitude of interaction parameters involved in the block copolymers. The endblock A with the smallest fraction forms the core cylinder, and its neighboring block B, which has a sufficient amount of volume to surround the A cylinder, forms the cylindrical shell in the C matrix. This morphology is very similar to the "cylinder in cylinder" microstructure as experimentally observed for PS-PB-PMMA triblock[10,11]. It has been known that this structure is realized under the condition of $\phi_A < \phi_B < \phi_C$ in ABC triblock copolymers[10,11].

A morphological change occurs when the length of block A is increased on the expense of that of block C at constant f_B, i.e., the block composition is changed from $A_{10}B_{20}C_{50}$ to $A_{20}B_{20}C_{40}$. As shown in Figure 2(a), the structure of $A_{20}B_{20}C_{40}$ triblock seems to be a cylinder-type morphology. Since the length of block A in $A_{20}B_{20}C_{40}$ triblock is increased compared to $A_{10}B_{20}C_{50}$ triblock, the cylindrical B domain cannot form the continuous shell around the A cylinder. In other words, the rupture of B shell occurs as a result of the increased volume fraction of block A, leading to the formation of favorable A/C contact. Therefore, cylinders of midblock B are formed at the interface between matrix and core cylinders. A similar morphology was experimentally observed by Stadler

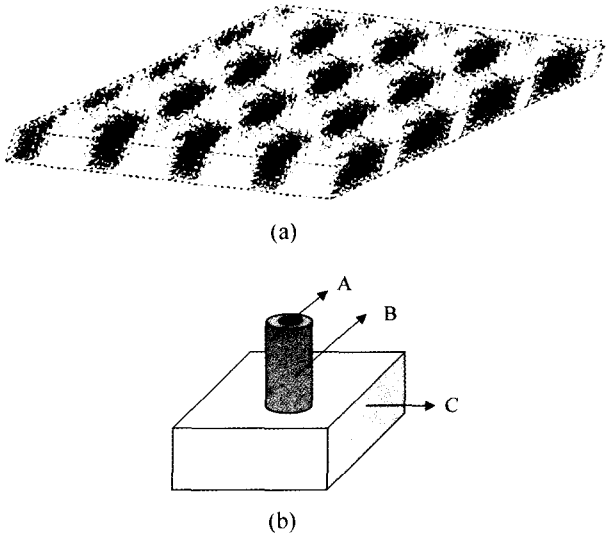

Figure 1. (a) Snapshot of $A_{10}B_{20}C_{50}$, where A, B, and C segments are colored black, gray, and white, respectively. A schematic description of the copolymer morphology is shown in (b).

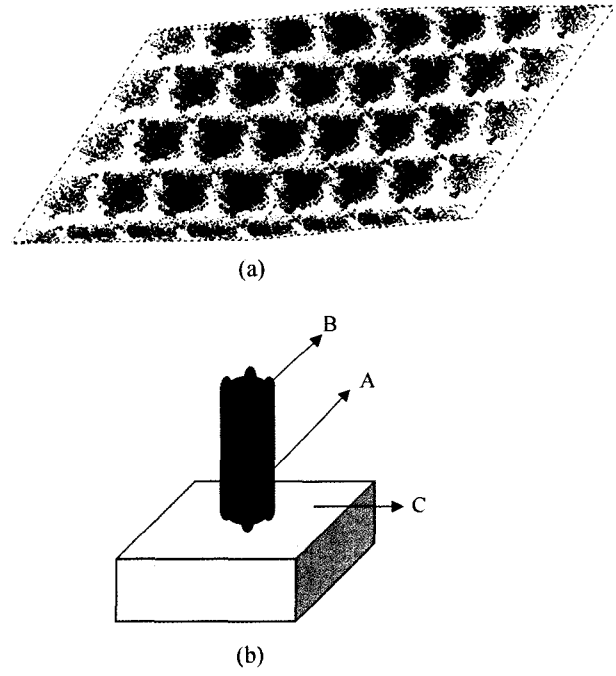

Figure 2. (a) Snapshot of $A_{20}B_{20}C_{40}$, where A, B, and C segments are colored black, red, and yellow, respectively. A schematic description of the copolymer morphology is shown in (b).

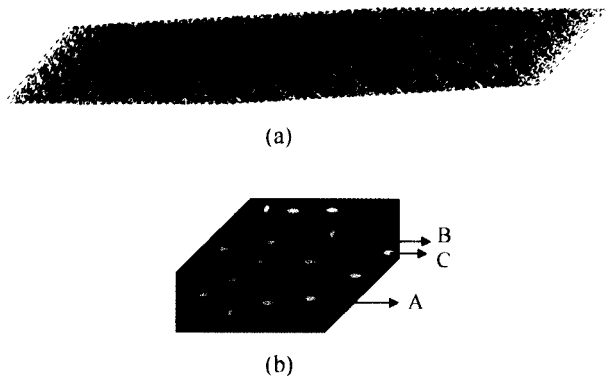

Figure 3. (a) Snapshot of $A_{50}B_{20}C_{10}$, where A, B, and C segments are colored black, red, and yellow, respectively. A schematic description of the copolymer morphology is shown in (b).

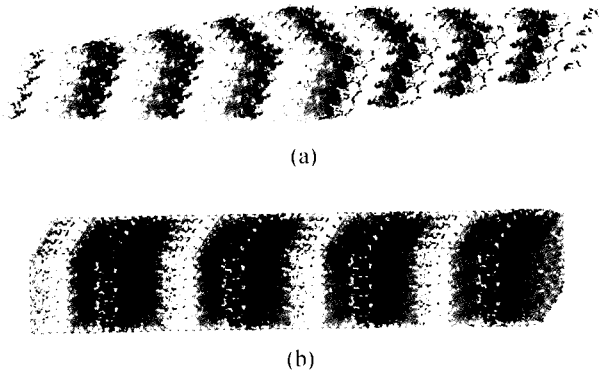

Figure 4. Snapshot of triblock copolymers with $f_B = 0.33$: (a) $A_{18}B_{26}C_{36}$; (b) $A_{36}B_{26}C_{18}$, where A, B, and C segments are colored black, gray, and white, respectively.

group[11]. They designated this structure as "cylinders at cylinder" structure. The transition from the "cylinder in cylinder" to "cylinders at cylinder" structure is achieved by increasing the ratio of volume fraction f_A/f_B.

When ABC triblock copolymers with the block A as a major component are simulated, it reveals that their morphologies exhibit totally different structures from those with the block A as a minor component at the same composition of midblock. The morphology simulated for the $A_{50}B_{20}C_{10}$ triblock copolymer is shown in Figure 3(a). The block A forms the matrix due to the larger volume fraction as compared to B and C blocks, while the B and C blocks seems to form the two kinds of spherical domains. This separation between dispersed phases occurs as a consequence of the unfavorable interaction between the midblock B and the endblock C. In other words, the morphology reduces unfavorable interfacial area between the B and C domains by forming separated domains and thus creates more favorable A/C interface. However, due to the direct connection of block B and C, these two domains cannot perfectly be separated with each other, as shown in Figure 3. This morphology corresponds to the "sphere on sphere" structure, i.e., small sphere forms on the surface of other sphere in matrix, as experimentally observed in asymmetric ABC triblock copolymers with small volume fraction of midblock[12].

The subtle variation of midblock composition in ABC triblock copolymer can lead to significant morphological change, as previously reported in our study[7]. When the midblock composition is increased from $f_B = 0.25$ in Figure 2 to $f_B = 0.33$ in Figure 4, the snapshot of triblock copolymer $A_{18}B_{26}C_{36}$ ($f_B = 0.33$) shows the three-phases and four-layered lamellae, as shown in Figure 4(a). When the length of endblock is exchanged each other, the lamellar structure is also observed for $A_{36}B_{26}C_{18}$ triblock, as shown in Figure 4(b). These lamellar structures are identified by the calculated scattering patterns, where characteristic Bragg-peaks of higher order are observed as the integer multiples of q^* (not shown here). When the length of block A is increased further, the morphology developed from $A_{42}B_{26}C_{12}$ triblock exhibits a different structure from the $A_{18}B_{26}C_{36}$ (Figure 4(a)) and $A_{36}B_{26}C_{18}$ (Figure 4(b)) triblocks in spite of the same composition of midblock, as can be seen in Figure 5(a). The

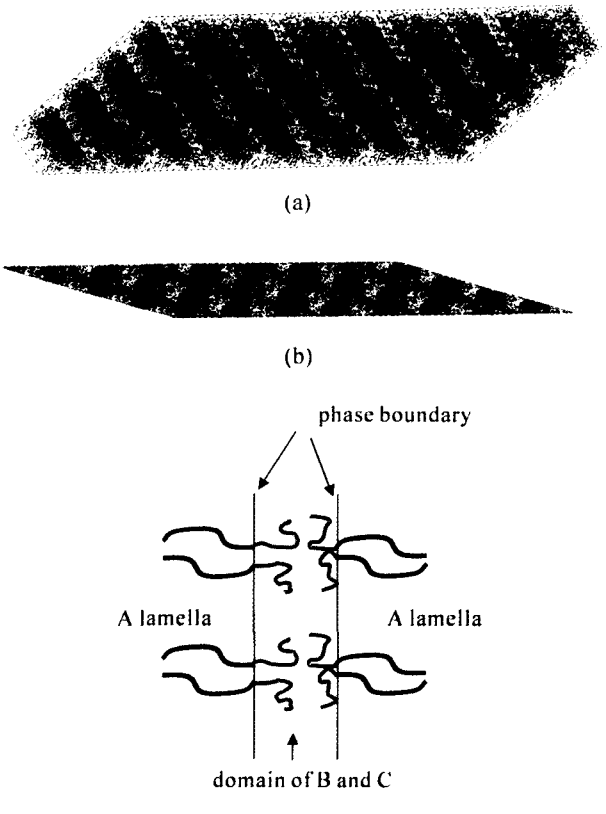

Figure 5. (a) Snapshot of $A_{42}B_{26}C_{12}$, where A, B, and C segments are colored black, red, and yellow, respectively. A birds-eye view of the simulation cell shown in (a) is presented in (b). Scheme of a possible arrangement of each block in triblocks is shown in (c).

overall morphology of $A_{42}B_{26}C_{12}$ is a lamellae which is composed of two layers. The A microdomain forms one layer while both the B and C microdomains form the other layer. In the latter layer, the B and C are phase-separated to form its own phase due to the repulsive interaction between B and C blocks. The bird's eye view of the simulation box in Figure 5(b) reveals this structure more clearly, and a possible arrangement of each block in the morphology is schematically shown in Figure 5(c).

The simulated results for triblock copolymers with $f_B = 0.5$ are shown in Figure 6. The snapshot of $A_{10}B_{40}C_{30}$ looks basically the lamellar-type structure. As shown in Figure 6(a), the lamella is formed from B and C blocks, while the microdomains from A block are located at the interface between B and C domain. Increasing the length of block A with keeping the length of midblock B constant, leads to a morphological transition. The morphology for $A_{25}B_{40}C_{15}$ triblock shows that two kinds of cylinders composed of two end blocks are formed in the B matrix, as shown in Figure 6(b). For clarity, the snapshot is redrawn in Figure 6(c) with the A and B blocks in $A_{25}B_{40}C_{15}$ triblock being removed from Figure 6b. Such a morphology, in which the midblock forms the matrix and two endblocks form cylindrical microdomain, has been experimentally observed in PB-PS-PMMA[14] and PI-PS-P2VP triblock copolymers[15]. It has been reported that the cylinders in these systems are arranged in a tetragonal pattern. On the other hand, Brinkmann *et al.*[19] recently reported that it was possible for two kinds of cylinders in PS-PB-PMMA triblock copolymers to pack in the hexagonal mode. These different reports on packing mode may arise from the difference of thermodynamic conditions between the systems. In the former triblock systems, i.e., PB-PS-PMMA or PI-PS-P2VP triblock, the interaction energy between two endblocks forming two kinds of cylinders is much larger than the one between each endblock and midblock. However, in PS-PB-PMMA with hexagonal packing mode, the interaction between two endblocks is relatively favorable. Since our simulation system resembles the PS-PB-PMMA triblock more closely, hexagonal packing of the cylindrical domain is expected, but the accurate packing mode cannot be realized in simulation due to the finite size of simulation box.

Finally, the composition effect is examined on the asymmetric triblock copolymers with $f_B = 0.625$. In the $A_{10}B_{50}C_{20}$ triblock, a novel morphology is observed, as shown in the snapshot of Figure 7(a). The microdomain of block A can be recognized as small microdomains at the phase boundary of the C cylinders and the B matrix, as schematically shown in Figure 7(b). Indeed, a similar morphology was experimentally observed in asymmetric PS-PB-PMMA triblock when $\phi_{PS} = 0.74$, $\phi_{PB} = 0.04$ and $\phi_{PMMA} = 0.22$[11]. This morphology is named as "spheres on cylinder" structure. The transition from "cylinders at cylinder" or "helical" structure to "spheres on cylinder" structure can be achieved by decreasing the ratio of ϕ_{PB}/ϕ_{PMMA}, i.e., the cylindrical PB domains, which are either arranged as straight cylinders or as helices around a PMMA cylinder, break into isolated PB particles[11]. The difference between our simulation and the experiments is that the PS

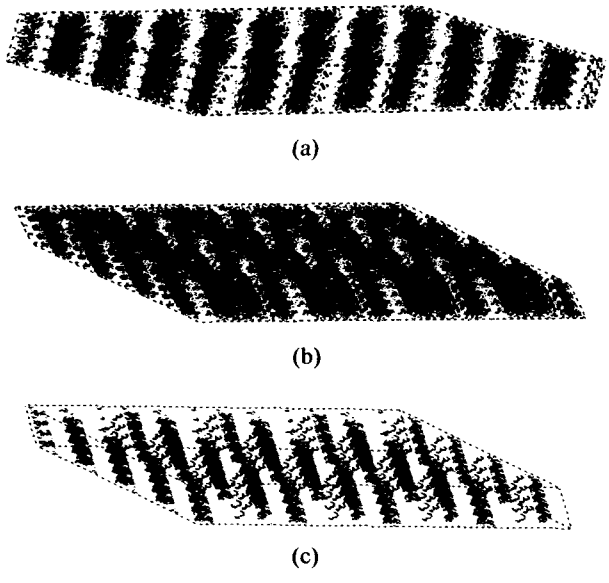

Figure 6. Snapshot of triblock copolymers with $f_B = 0.5$: (a) $A_{10}B_{40}C_{30}$; (b) $A_{25}B_{40}C_{15}$. For clarity, the snapshot is redrawn in (c) with A and B segments being removed from (b).

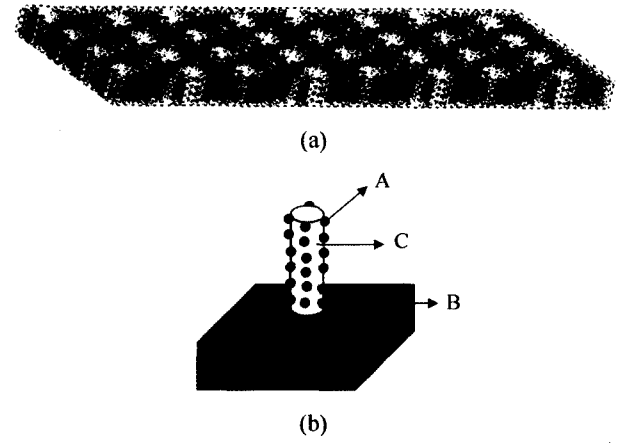

Figure 7. (a) Snapshot of $A_{10}B_{50}C_{20}$, where A, B, and C segments are colored black, red, and yellow, respectively. A schematic description of the copolymer morphology is shown in (b).

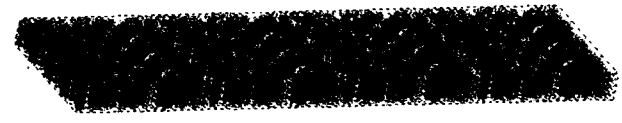

Figure 8. Snapshot of $A_{20}B_{50}C_{10}$, where A, B, and C segments are colored black, red, and yellow, respectively.

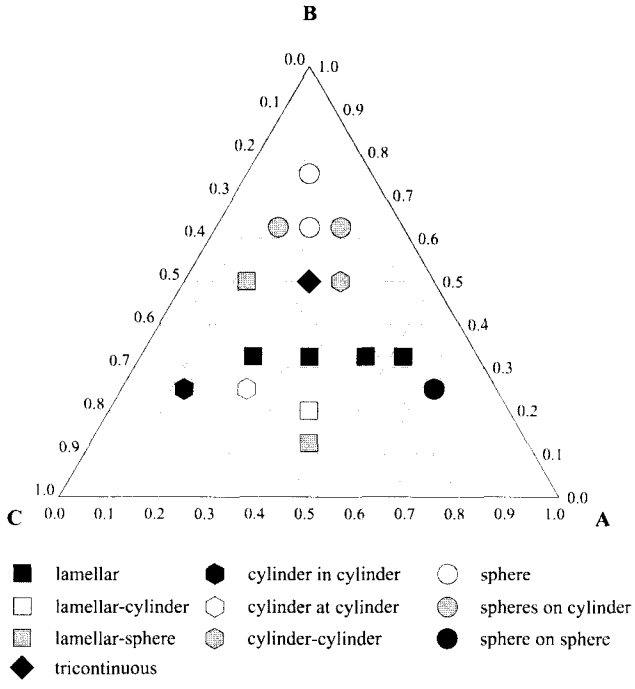

Figure 9. Phase diagram of ABC triblock copolymers under the condition of $\chi_{AC} < \chi_{AB} < \chi_{BC}$.

endblock forms the matrix in experiment whereas the B midblock forms the matrix in our simulation. In both cases, the composition of each block and thermodynamic imbalance between midblock and endblocks are important factors to determine the morphology. In the case of $A_{20}B_{50}C_{10}$ triblock, a similar morphology to the case of $A_{20}B_{50}C_{10}$ is also observed, as shown in Figure 8.

Conclusions

In this study, the effect of block composition on the morphology of asymmetric ABC triblock copolymers was investigated using a molecular dynamics simulation. Our simulation shows that unlike symmetric ABC triblock copolymers, more fascinating morphologies are observed in asymmetric ones because of a larger difference of incompatibility between the components. With changing the composition of endblock at a given value of $f_B = 0.25$, the transition from the "cylinder in cylinder" to the "cylinders at cylinder" structure was observed in our simulation. In the case of ABC triblocks with $f_B = 0.5$, lamellar-type structure is changed to cylinder-type structure with increasing the length of block A. When the midblock length increases further to $f_B = 0.625$, the "spheres on cylinder" structure is observed in both the $A_{10}B_{50}C_{20}$ and $A_{20}B_{50}C_{10}$ triblocks.

The phase diagram of ABC triblock copolymers can be constructed from simulation results including both the symmetric and asymmetric cases, under the condition of our simulation, i.e., $\varepsilon_{AC} < \varepsilon_{AB} < \varepsilon_{BC}$, which corresponds to $\chi_{AC} < \chi_{AB} < \chi_{BC}$ in ABC triblock copolymers. As shown in Figure 9, it is evident that with increasing the value of f_B, the morphology of the ABC triblock copolymer changes from the lamellar structures to the cylindrical domains and finally to the spherical domains. Most of simulated morphologies of ABC triblock copolymers are evidenced by experimental results, and therefore our simulation method provides us with a guideline for designing new microphase morphology by tailoring triblock copolymers.

Acknowledgement

The authors thank the Korea Science and Engineering Foundation (KOSEF) for their financial support through the Hyperstructured Organic Materials Research Center (HOMRC).

References

1. D. A. Hajduk, P. E. Harper, S. M. Gruner, C. C. Honeker, G. Kim, E. L. Thomas, and L. J. Fetter, *Macromolecules*, **27**, 4063 (1994).
2. T. Hashimoto, M. Shibayama, and H. Kawai, *Macromolecules*, **13**, 1237 (1980).
3. T. P. Russell, T. E. Karis, Y. Gallot, and A. M. Mayes, *Nature*, **368**, 729 (1994).
4. L. Leibler, *Macromolecules*, **13**, 1602 (1980).
5. M. Matsen and F. S. Bates, *Macromolecules*, **29**, 1092 (1996).
6. M. Matsen and F. S. Bates, *J. Chem. Phys.*, **106**, 1997 (1997).
7. M. J. Ko, S. H. Kim, and W. H. Jo, *Macromol. Theory Simul.*, **10**, 381 (2001).
8. M. J. Ko, S. H. Kim, and W. H. Jo, *Fibers and Polymers*, **3**, 8 (2002).
9. R. Stadler, C. Auschra, J. Beckmann, U. Krappe, I. Voigt-Martin, and L. Leibler, *Macromolecules*, **28**, 3080 (1995).
10. U. Krappe, R. Stadler, and I. Voigt-Martin, *Macromolecules*, **28**, 4558 (1995).
11. U. Breiner, U. Krappe, V. Abetz, and R. Stadler, *Macromol. Chem. Phys.*, **198**, 1051 (1998).
12. U. Breiner, U. Krappe, T. Jakob, V. Abetz, and R. Stadler, *Polym. Bull.*, **40**, 219 (1998).
13. V. Abetz and R. Stadler, *Macromol. Symp.*, **113**, 19 (1997).
14. K. Jung, A. Volker, and R. Stadler, *Macromolecules*, **29**, 1076 (1996).
15. Y. Mogi, M. Nomura, H. Kotsuji, K. Ohnishi, Y. Matsushita, and I. Noda, *Macromolecules*, **27**, 6755 (1994).
16. Y. Mogi, H. Kotsuji, Y. Kaneko, K. Mori, Y. Matsushita, and I. Noda, *Macromolecules*, **25**, 5408 (1992).
17. Y. Mogi, H. Kotsuji, K. Ohnishi, Y. Matsushita, and I. Noda, *Macromolecules*, **25**, 5412 (1992).
18. S. P. Gido, D. W. Schwark, E. L. Thomas, and M. D. Goncalves, *Macromolecules*, **26**, 2636 (1993).
19. S. Brinkmann, R. Stadler, and E. L. Thomas, *Macromolecules*, **31**, 6566 (1998).